JOURNAL OF CATALYSIS **158,** 51–63 (1996)
ARTICLE NO. 0005

Reforming of Methane with Carbon Dioxide to Synthesis Gas over Supported Rhodium Catalysts

I. Effects of Support and Metal Crystallite Size on Reaction Activity and Deactivation Characteristics

Z. L. Zhang, V. A. Tsipouriari, A. M. Efstathiou, and X. E. Verykios

Department of Chemical Engineering and Institute of Chemical Engineering and High Temperature Processes, University of Patras, P.O. Box 1414, GR-26500 Patras, Greece

Received September 1, 1994; revised May 3, 1995; accepted August 25, 1995

The effects of carrier and metal particle size on the catalytic performance (initial intrinsic activity and deactivation characteristics) of Rh in the reaction of reforming of methane with carbon dioxide were investigated. The specific activity of Rh catalysts was found to strongly depend on the carrier employed to disperse the metal, decreasing in the order yttria-stabilized zirconia (YSZ) > Al_2O_3 > TiO_2 > SiO_2 > La_2O_3 > MgO, a result which correlates directly with the acidity characteristics of the carrier. The initial intrinsic activity and rate of deactivation of Rh were also found to be sensitive to the metal particle size, in the range 1 ~ 6 nm. Both activity and rate of deactivation were found to decrease with increasing metal particle size. However, the degree of these dependences was found to be largely affected by the nature of the carrier, suggesting that the dependence of activity and rate of deactivation on metal particle size is likely to be related to metal–support interactions. While relatively high deactivation rates were observed over Rh supported on TiO_2 and MgO, lower deactivation rates were observed over Rh supported on YSZ, Al_2O_3, La_2O_3, and SiO_2. Evidence was found that at least three kinds of factors contribute to catalyst deactivation, namely, carbon deposition, metal sintering, and poisoning of surface Rh sites by species originating from the carrier. The importance of each of these factors was found to be determined by the nature of the carrier.

INTRODUCTION

Conversion of methane and carbon dioxide, which are two of the most abundant carbon-containing materials, into useful products is an important area of current catalytic research. The reforming reaction of methane with carbon dioxide to synthesis gas (CO/H_2) is a very attractive route for the production of energy and chemicals (1, 2). As already discussed in the literature, this reaction offers important advantages over the process of steam reforming of methane, namely, (a) the formation of a suitable H_2/CO ratio for use in Fischer–Tropsch synthesis to liquid hydrocarbons, (b) utilization of CO_2, which is a greenhouse gas, and (c) better use in chemical energy transmission systems (3–5).

The reforming reaction of methane with carbon dioxide was first studied by Fischer and Tropsch (6) using nickel- and cobalt-based catalysts. Since then, a large number of catalysts has been tested and it has been demonstrated that most of the Group VIII metals are more or less catalytically active towards this reaction. Conversions of CH_4 and CO_2 to synthesis gas approaching those defined by thermodynamic equilibrium can be obtained over most of the aforementioned catalysts as long as contact times are kept high enough (7–10). One of the major problems encountered towards application of this process is deactivation of the catalyst by carbon deposition.

Although development of catalysts based on nonnoble metals (e.g., Fe, Co, Ni) is of interest from the industrial point of view, the results obtained so far have shown that rapid deactivation is experienced over such catalysts. In some extreme cases the deactivation rate is so high that catalytic activity is completely lost within a few hours of reaction. This is presumably due to the formation of stable and inactive carbon (e.g., Ni carbide) on the surface (9). Failure to develop a nonnoble metal catalyst with long-term stable performance is, to a large extent, attributed to the limited knowledge concerning activation of methane and carbon dioxide over supported metal crystallites, the properties of which are significantly affected by the metal particle size and the nature of the support. On the other hand, noble metal catalysts exhibit better activity and suffer less from carbon deposition as compared to nonnoble metal catalysts (9, 11). Recently, numerous studies (11–16) related to the reforming reaction of methane with carbon

0021-9517/96 $12.00

dioxide have been conducted over noble metals in order to develop a successful catalyst and to gain an enhanced understanding of the mechanisms of reaction and deactivation.

Richardson and Paripatyadar (11) have compared the catalytic performance of $Rh/\gamma\text{-}Al_2O_3$ and $Ru/\gamma\text{-}Al_2O_3$ catalysts for the reforming reaction of CH_4 with CO_2. They found that the two catalysts have comparable activities, while the $Rh/\gamma\text{-}Al_2O_3$ catalyst exhibits better stability than the $Ru/\gamma\text{-}Al_2O_3$. Ashcroft *et al.* (12) have tested various noble metals for the CO_2 reforming and found that activity decreases in the order Ir > Rh > Ru > Pd. However, a somewhat different activity order was reported by Solymosi *et al.* (13), who observed that Ru and Pd were the most active among Pd, Ru, Rh, Pt, and Ir. These differences among the two research groups are likely to be the result of the different basis of activity evaluation. Solymosi's group (13) has reported specific activities based on the exposed metal atoms, which is not the case for the other research group (12). Rostrup-Nielsen and Hansen (14) have recently studied the CO_2 reforming over catalysts based on Ni, Ru, Rh, Pd, Ir, and Pt. They observed that Ru and Rh show high selectivity for carbon-free operation. The influence of the catalyst support on the catalytic performance of CO_2 reforming over Rh and Pd crystallites was studied by Erdöhelyi *et al.* (15, 16) and Nakamura *et al.* (17). The former group reported that there exists no carrier effect for supported Rh catalysts (except for MgO support), but a significant carrier effect occurs for supported Pd catalysts. On the other hand, the latter group observed that the specific activity over Rh crystallites is significantly affected by the nature of the carrier.

The present work reports results of an investigation of the effects of support (TiO_2, $\gamma\text{-}Al_2O_3$, MgO, SiO_2, La_2O_3, and yttria-stabilized zirconia (YSZ)) and metal crystallite size (1 ~ 10 nm) of Rh-supported catalysts on their methane reforming activity in the temperature range 600–800°C. Parameters such as the alteration of metal dispersion with reaction time, the amount of active and inactive carbon species formed on the working catalyst surface, and causes of catalyst deactivation were particularly studied. In Part 2 of this work (18), various transient isotopic techniques were used in order to obtain information on the surface coverages of adsorbed carbon- and oxygen-containing species formed during reaction over the Rh/YSZ and Rh/Al_2O_3 catalysts. It is hoped that this work can lead to an enhanced understanding of the reaction mechanism of CO_2 reforming and also of the effects of support on catalyst deactivation.

EXPERIMENTAL

(*a*) *Catalyst Preparation and Characterization*

The carriers employed for the preparation of rhodium catalysts were SiO_2 (Alltech Associates), $\gamma\text{-}Al_2O_3$ (Akzo Chemicals), TiO_2 (Degussa, P-25), La_2O_3 (Alfa Products), MgO (Alfa Products), and yttria-stabilized zirconia, YSZ (CERECO). Catalysts were prepared by the method of incipient wetness impregnation using $RhCl_3 \cdot 3H_2O$ as the precursor compound. Weighed amounts of $RhCl_3 \cdot 3H_2O$ were dissolved in 10 ml of distilled water at 25°C, while 5 ~ 10 g of the carrier were added to the solution under continuous stirring at 25°C. The resulting suspension was then heated at 80°C to evaporate the water and the solid material was dried in an oven at 110°C for 24 h. The resulting material was subsequently treated with hydrogen at 200°C for 2 h and stored until further use. For catalytic studies, the fresh sample was heated under He to 500°C, reduced in H_2 for 2 h at the same temperature, followed by He purge and heating under He flow to the reaction temperature.

Metal dispersion of fresh catalysts, following H_2 reduction at 400°C for 2 h, was determined by static equilibrium H_2 adsorption at room temperature, following standard procedures. The alteration of metal dispersion with time of reaction was studied by H_2 chemisorption followed by temperature-programmed desorption (TPD), before and after reaction. This procedure was as follows. After the catalyst was exposed to the reaction conditions, the feed was switched to He for 3 min and then to O_2 for 15 min at 650°C in order to remove any carbon accumulated during reaction. The catalyst sample was then rapidly cooled to 300°C, exposed to H_2 flow for 1 h, and then cooled to 30°C and maintained for 30 min under H_2 flow. The feed was subsequently switched to He and a H_2 TPD was initiated, measuring the desorbing H_2 with on-line mass spectrometry. A similar experiment as the one described above but without the 15-min oxygen treatment of the catalyst was performed over the Rh/MgO which accumulated only very small amounts of carbon. It was found that the 15-min oxygen treatment had only a very small effect (<5%) on H_2 chemisorption. The surface carbon species formed on the working catalyst surface were studied by temperature-programmed oxidation (TPO). These experiments and those of H_2 chemisorption/TPD described above were conducted in a specially designed flow system which has been described elsewhere (19). Chemical analysis of gaseous streams during TPD and TPO was done by an on-line mass spectrometer (VG Quadrupoles, SXP Elite) equipped with fast response inlet capillary and data acquisition systems.

(*b*) *Catalyst Testing*

Kinetic studies under differential conditions and studies under integral reactor conditions at atmospheric pressure were conducted in a conventional flow apparatus consisting of a flow measuring and control system, a mixing chamber, a quartz fixed-bed reactor, and an on-line gas chromatograph. Flow rates were monitored and controlled by ther-

mal mass flow meters (MKS Instruments). In the case of integral reactor performance studies, significant temperature gradients along the catalyst bed and between the gas and solid surfaces have been experienced. On the other hand, such temperature gradients became significantly smaller under differential reactor performance studies. In order to minimize heat transport effects, the supported Rh catalyst (one portion) was diluted with α-Al_2O_3 or SiO_2 (four portions). It was estimated that under differential reactor conditions and using a feed mixture of 20% CH_4, 20% CO_2, and 60% He, the temperature gradients were not greater than 10°C. Interphase and intraparticle diffusional resistances were strictly limited under these conditions. The temperature of the catalyst was measured by a chromel–alumel thermocouple placed in the middle of the catalyst bed.

The quartz reactor diameter used was 3 mm i.d., the total flow rate was varied between 50 and 400 cc STP/min, the catalyst particle diameter was less than 0.02 mm, and the catalyst bed height was between 3 and 5 mm. Analysis of the feed stream and reaction mixture was performed using the TC detector of the gas chromatograph. A Carbosieve S-II 100/120 column was used to separate H_2, N_2, CO, CH_4, CO_2, and H_2O. Prior to reaction, a reduction of all catalysts at 500°C in H_2 flow for 1 h was applied, except for Rh/TiO_2 which was reduced at 300°C so as to avoid inducing the SMSI state.

The methane and carbon dioxide gases used were of high purity (>99.99%), while the He gas was standard (99.95%). Further purification of He gas was performed through molecular sieve and MnO_x traps. Mass spectrometric analysis of the 20% CH_4/20% CO_2/He mixture resulted in no detectable (<1 ppm) H_2S and SO_2 gas.

RESULTS

The results of the effects of metal particle size (d = 1 ~ 10 nm) and support (TiO_2, γ-Al_2O_3, MgO, SiO_2, La_2O_3, and yttria-stabilized zirconia (YSZ)) on the catalytic performance of Rh crystallites obtained under differential conditions are first presented, followed by results of long-term stability testing of selected supported Rh catalysts under integral reactor conditions, in the temperature range 600–800°C.

(*a*) *Kinetic Studies* (*Differential Reactor Performance*)

1. Effects of metal particle size. The effect of particle size, or degree of dispersion, on the initial intrinsic activity of Rh for the methane reforming reaction with CO_2 was investigated over Rh/Al_2O_3, Rh/SiO_2, and Rh/TiO_2 catalysts. Different dispersions were achieved by varying the metal loading between 0.2 and 10 wt%. Figure 1 shows the variation of the turnover frequency (TOF) with the average Rh particle size, at 650°C. TOF values correspond to initial activity obtained by extrapolation of TOF vs time of reaction curves to zero time. It is apparent from the results shown in Fig. 1 that structure sensitivity of this catalytic system strongly depends on the carrier employed to disperse the metal. The Rh/TiO_2 catalyst exhibits strong structure sensitivity, where the TOF decreases with increasing Rh particle size in the range 1 to 5 nm. On the other hand, the Rh/Al_2O_3 catalyst shows a moderate structure sensitivity, while the Rh/SiO_2 catalyst exhibits a facile behavior. These results are in good agreement with the facts that small metal particles are strongly amenable to metal–support interactions; TiO_2 is considered to be one of the most interactive carriers, while SiO_2 is one of the most inert.

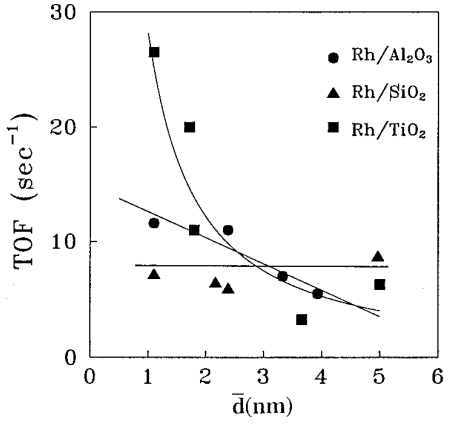

FIG. 1. Dependence of initial specific activity (TOF) of the CH_4/CO_2 reaction on the average Rh particle size of Rh/Al_2O_3, SiO_2, and TiO_2 catalysts. T = 650°C; P_{CH_4} = 0.2 bar; CH_4/CO_2 = 1.0.

The influence of Rh particle size on the rate of deactivation over Rh/Al_2O_3, Rh/SiO_2, and Rh/TiO_2 catalysts was also investigated at 650°C and results are shown in Fig. 2.

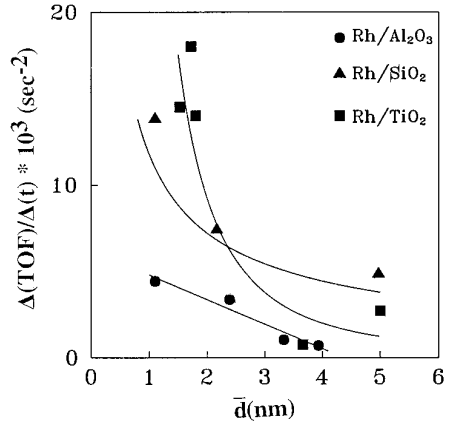

FIG. 2. Dependence of deactivation rate of the CH_4/CO_2 reaction on the average Rh particle size of Rh/Al_2O_3, SiO_2, and TiO_2 catalysts. T = 650°C; P_{CH_4} = 0.2 bar; CH_4/CO_2 = 1.0.

TABLE 1

Effect of Support on the Initial Activity (TOF) of CH_4 Reforming with CO_2 over Supported Rh Catalysts with 0.5 wt% Rh at 650°C: P_{CH_4} = 0.2 bar, P_{CO_2} = 0.2 Bar

Catalyst support for 0.5 wt% Rh	Dispersion[a] (%)	$\bar{d}$ (nm)	TOF (s^{-1})	E[b] (kJ/mol)
YSZ	45	2.5	60.0	—
Al_2O_3	100	2.4	11.5	94.5
TiO_2	75	2.5	10.0	84.4
SiO_2	100	2.4	6.0	84.9
La_2O_3	20	5.5	6.0	—
MgO	50	2.2	0.8	—

[a] Metal dispersion was measured by H_2 chemisorption at room temperature over fresh samples as described in the text (D = 100% corresponds to 2.2 m^2 Rh/g_{cat}).

[b] Activation energy was measured in the temperature range 500–650°C.

Results are presented in terms of $\Delta(TOF)/\Delta t$, a parameter which was obtained from the linearly decreasing part of TOF vs time curves, at short reaction times (21). As a general tendency, a reduction of Rh particle size results in an enhanced rate of deactivation. It appears that the enhanced rate of deactivation over small metal crystallites may be related to one or more of the following factors: (a) increased availability of low coordination metal sites over which carbon deposition is favored (20), (b) enhanced degree of Rh metal sintering, and (c) increased extent of participation of the catalyst carrier, which could promote carbon deposition on the metallic sites, and/or block metal active sites. In a following section, these three possible factors, which may be responsible for the behaviour shown in Fig. 2, are addressed.

2. Effects of catalyst carrier. The effect of catalyst carrier on the initial specific activity (TOF), which was obtained by extrapolation of TOF vs time of reaction curves to zero time, was investigated by varying the carrier among γ-Al_2O_3, TiO_2, SiO_2, La_2O_3, MgO, and YSZ. The values of TOF obtained over various catalysts corresponding to a given metal particle size ($\bar{d}$) are reported in Table 1, in which the metal dispersion of the fresh 0.5 wt% Rh-supported catalysts, and the apparent activation energy of reaction, obtained within the temperature range 500 to 650°C, are also reported. It is shown that the methane reforming activity of Rh decreases in the following order: YSZ > Al_2O_3 ≥ TiO_2 > SiO_2 > La_2O_3 > MgO. The highest initial rate observed over Rh/YSZ, is nearly 80 times larger than the rate obtained over Rh/MgO. Note that the average Rh particle size of the Rh/YSZ and Rh/MgO catalysts employed in these measurements does not differ significantly, as shown in Table 1. Thus, the differences in the initial values of TOF obtained over these supported Rh catalysts cannot be attributed to differences in Rh particle size. It is apparent that a strong carrier effect on the initial activity of supported Rh crystallites exists. The apparent activation energies obtained over Rh supported on γ-Al_2O_3, TiO_2 and SiO_2 were in the range of 85–95 kJ/mol, indicating only a weak support effect. This result is in good agreement with values reported in previous studies (14, 15).

The deactivation characteristics of Rh supported on various carriers was also quantified by calculating the ratio of the rate of reaction after 500 min on stream over that after 10 min on stream. Values of this deactivation index are shown in Table 2. These values are relatively high when Rh is dispersed on γ-Al_2O_3, YSZ, La_2O_3, and SiO_2, and rather low when Rh is dispersed on TiO_2 and MgO, revealing that the catalyst carrier also affects the kinetics of deactivation of Rh crystallites (see also Fig. 2). It must also be noted that there is no direct correlation between specific catalytic activity and extent of deactivation (see Table 1). In many previous studies (11, 12), catalyst deactivation was attributed to surface carbon deposition due to the Boudouard reaction, and/or methane cracking. However, sintering of the metal crystallites may also contribute to catalyst deactivation, given the fact that the reaction temperature is high (>600°C). Possible causes of catalyst deactivation were explored by investigating the variation of surface carbon and average Rh crystallite size with time on stream.

The quantity of adsorbed carbon-containing species (except that of CO and CO_2) formed during the CH_4/CO_2 reforming reaction at 650°C, and its reactivity towards oxygen and hydrogen were studied with the following methodology. Following reaction for a certain period of time, t, the reactor was purged with He at 650°C for 10 min, and then was cooled quickly in He flow to 100°C. The feed was subsequently changed to either 10% O_2/He or pure H_2 and the temperature was increased at a rate of 20°C/min to

TABLE 2

Effect of Support on the Deactivation Characteristics of Supported Rh Catalysts Containing 0.5 wt% Rh

Catalyst support 0.5 wt% Rh	$r_{500\ min}/r_{10\ min}$	θ_c (monolayers)[a] t = 10 min	θ_c (monolayers)[a] t = 2 h
Al_2O_3	0.7	0.64	0.60
YSZ	0.7	0.003	0.03
TiO_2	0.3	0.008	0.007
SiO_2	0.8	—[b]	—[b]
La_2O_3	0.7	—[b]	—[b]
MgO	0.3	0.03	0.03

[a] Equivalent amount of carbon in monolayers of surface Rh atoms (C/Rh_S = 1) as determined by TPO experiments.

[b] Not measured.

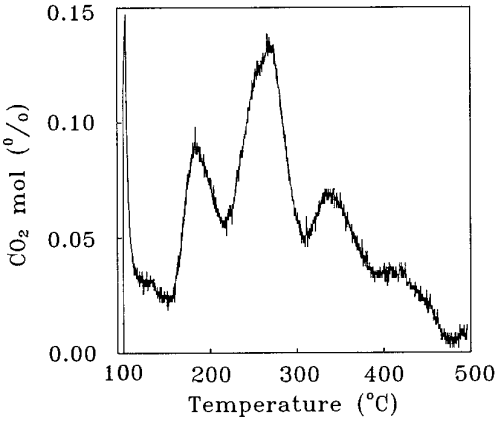

FIG. 3. Temperature-programmed oxidation (TPO) of carbon species formed after 10 min of reaction with CH_4/CO_2 over the 0.5 wt% Rh/Al_2O_3 catalyst. $T = 650°C$; $\beta = 20°C/min$; $P_{CH_4} = 0.2$ bar; $CH_4/CO_2 = 1.0$.

carry out a temperature-programmed oxidation (TPO) or hydrogenation (TPH) experiment.

Figure 3 shows the CO_2 response obtained during TPO over the 0.5 wt% Rh/Al_2O_3 catalyst after reaction at 650°C for 10 min. At the conditions of the experiment performed, it is possible to distinguish four peaks with maxima at $T = 100$, 180, 270, and 330°C. An approximate deconvolution of the CO_2 spectrum shown in Fig. 3 provides the amount of each of the four carbon species formed. These carbon species are designed as C_α, C_β, C_γ, and C_δ, in accordance with their reactivity order, and their amounts are found to be 1.9, 5.8, 14.6, and 8.7 $\mu mol/g_{cat}$, respectively. The total amount of carbon deduced from the TPO experiment of Fig. 3 is 31.0 $\mu mol/g_{cat}$, which corresponds to an equivalent amount of monolayers, θ_c, based on the Rh surface alone, of 0.6 (assuming $C/Rh_S = 1$). Similar TPO experiments for different reaction times revealed that the proportion of each type of carbon (C_α, C_β, C_γ, and C_δ) is altered to a certain extent with time on stream. For instance, the sharp C_α peak is reduced as reaction time increases from 10 min to 2 h, suggesting that some transformation of active carbon to a less active form occurs. This aspect is also illustrated through TPH experiments which are described below.

Figure 4 presents the CH_4 responses versus reaction temperature obtained during TPH, following reforming reaction at 650°C for 2 min (Fig. 4a) and 2 h (Fig. 4b) on stream over the 0.5 wt% Rh/Al_2O_3 catalyst. Three well resolved CH_4 peaks are observed in Fig. 4a. The first sharp peak ($T_M = 100°C$) corresponds to the hydrogenation of a very active carbon species. A second kind of carbonaceous species, the most abundant one, is hydrogenated in the range 130–320°C. As time on stream increases, the hydrogenation of this second kind of carbon species takes place at higher temperatures and its quantity decreases (compare Figs. 4a and 4b). This result suggests that ageing of this kind of carbon species occurs with time on stream, a result also observed during TPO experiments. A third small CH_4 peak is also obtained in the range 350–500°C ($T_M = 400°C$, Fig. 4a) corresponding to a less active carbonaceous species as compared to the ones described before. The amounts of carbonaceous species determined by the TPH experiment are found to correspond to θ_C of 0.4 and 0.26 after 2 min and 2 h on stream, respectively. No higher hydrocarbons were measured during TPH for the experiments of Fig. 4.

Figure 5 presents results of a similar TPH experiment performed over the 0.5 wt% Rh/YSZ catalyst following the reforming reaction for 2 h. In addition to methane, ethane is also formed, as indicated in Fig. 5. However, the

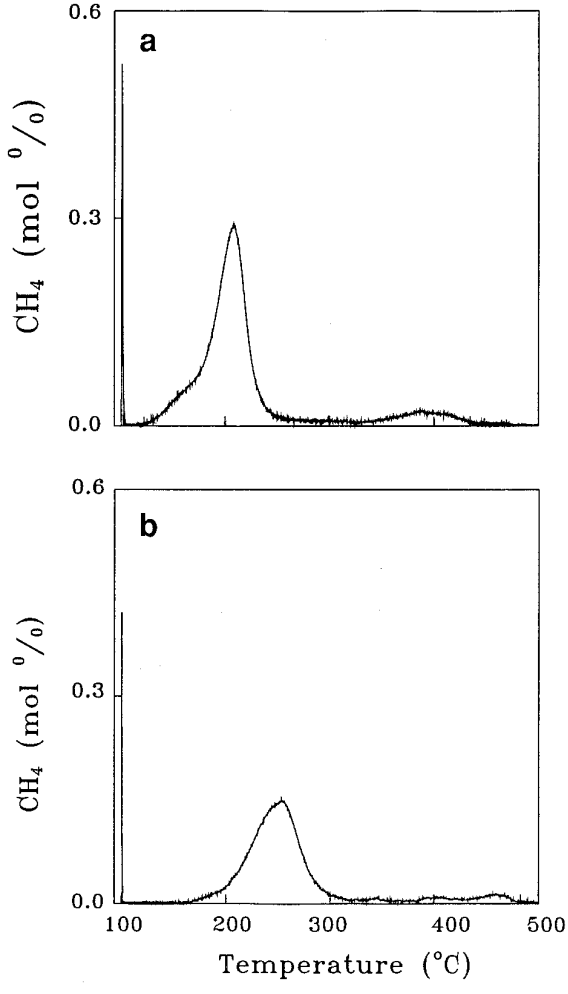

FIG. 4. Temperature-programmed hydrogenation (TPH) of carbon species formed during reforming reaction of CH_4 with CO_2 at 650°C over the 0.5 wt% Rh/AL_2O_3 catalyst. Gas delivery sequence: CH_4/CO_2/He (650°C, Δt) → He (650°C, 10 min) → cool in He flow to 100°C → H_2 (TPH), $\beta = 20°C/min$. (a) $\Delta t = 2$ min, (b) $\Delta t = 2$ h. Amount of sample used $W = 0.5$ g; $Q = 30$ ml/min (ambient).

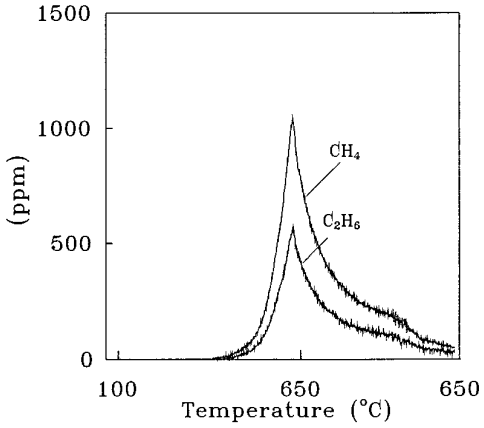

FIG. 5. Temperature-programmed hydrogenation (TPH) of carbon species formed during the reforming reaction of CH_4 with CO_2 at 650°C over the 0.5 wt% Rh/YSZ catalyst. Gas delivery sequence: CH_4/CO_2/He (650°C, 2 h) → He (650°C, 10 min) → cool in He flow to 100°C → H_2 (TPH), β = 20°C/min. Amount of sample used W = 0.5 g; Q = 30 ml/min (ambient).

hydrogenation characteristics of the carbonaceous species formed after the reforming reaction over the Rh/YSZ catalyst are very different from those observed over the Rh/Al_2O_3 catalyst. In the case of Rh/YSZ catalyst the reactivity of carbonaceous species towards hydrogenation is much lower than that of Rh/Al_2O_3, since in this case, production of CH_4 and C_2H_6 starts above 500°C (Fig. 5). Furthermore, the amount of carbonaceous species formed after 2 h on stream over the Rh/YSZ corresponds to θ_C of 0.03 to be compared with θ_C of 0.26 over the Rh/Al_2O_3 catalyst, both determined by TPH.

Figure 6 presents results of a transient isothermal oxidation experiment at 650°C performed over the Rh/MgO catalyst following reforming reaction for 2 h and a 10-min He purge at 650°C. Upon switching to the 10% O_2/He mixture, a rapid increase of the rate of oxidation of carbonaceous species to CO_2 followed by a slow decay which lasts for about 10 min is obtained (Fig. 6). Note also a shoulder developed in the CO_2 response of Fig. 6 during the first 2 min of the transient. Integration of the CO_2 response shown in Fig. 6 provides an amount of θ_C of 0.03.

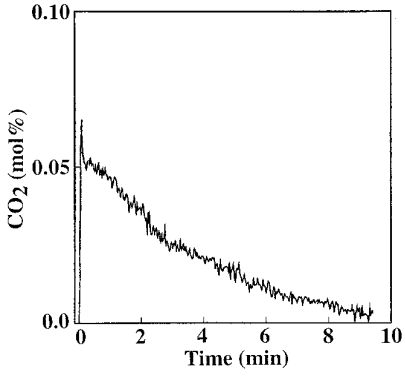

FIG. 6. Transient isothermal gas-phase response of CO_2 according to the gas delivery sequence CH_4/CO_2/He (650°C, 2 h) → He (650°C, 10 min) → 10% O_2/He (650°C, t) over the 0.5 wt% Rh/MgO catalyst. Amount of sample used W = 0.5 g; Q = 30 ml/min (ambient).

The total amount of carbon accumulated over various supported Rh catalysts after 10 min and 2 h of reaction time, as determined by TPO experiments, is reported in Table 2. Except for the Rh/Al_2O_3 catalyst, the amount of carbon formed on the other catalysts is very small ($\theta_C \leq$ 0.03). It is interesting to note that the amount of carbon accumulated on all the Rh catalysts is nearly independent of reaction time (the amount of carbon, θ_C, formed on the Rh/YSZ catalyst increases from 0.003 to 0.03 as reaction time increases from 10 min to 2 h but remains very small). Based on these results it could be argued that catalyst deactivation of Rh/TiO_2, Rh/YSZ, and Rh/MgO, which accumulate a very low amount of surface carbon with time on stream, is not mainly due to carbon deposition but to other surface processes.

The process of metal sintering (variation of the average Rh crystallite size with time on stream) was investigated with the following methodology. After the catalyst was exposed to the reaction mixture at 650°C for a specific period of time, the feed was switched to He for 3 min and then to O_2/He for 15 min in order to remove the carbon accumulated during reaction. The catalyst was rapidly cooled to 300°C, exposed to H_2 flow for 1 h, and then cooled to 30°C and maintained for 30 min under H_2 flow. The feed was subsequently switched to He and a H_2 TPD was initiated (β = 35°C/min). Before the TPD run, the reactor was flushed with He at 30°C for 5 min, time sufficient to remove the gas phase H_2 from the reactor and the lines. The quantity of H_2 desorbed was used to estimate the average Rh particle size. The above methodology resulted in approximately the same Rh particle size for the fresh sample (i.e., before reaction) as that obtained by the standard static equilibrium adsorption of H_2 at room temperature (see Experimental Section). This observation implies that the treatment which was applied in order to remove surface carbon and reduce the catalyst prior to H_2 chemisorption did not alter, to any significant extent, the dispersion of the catalysts.

Table 3 shows the alteration of average Rh crystallite size with time on stream, following reaction at 650°C over Rh/Al_2O_3, YSZ, TiO_2, and MgO catalysts. It is apparent that a substantial reduction of Rh dispersion occurs under the stated reaction conditions in the case of Rh/Al_2O_3. The degree of sintering, however, is significantly smaller for the Rh/TiO_2 catalyst, and is negligible for the Rh/YSZ and Rh/MgO catalysts. Therefore, sintering of the Rh particles of the Rh/Al_2O_3 and Rh/TiO_2 catalysts under

TABLE 3

Alteration of Average Rh Particle Size with Reaction Time, Δt, in $CH_4/CO_2/He$ Mixture at 650°C as a Function of Support for Various Supported Rh Catalysts Containing 0.5 wt% Rh

Catalyst support for 0.5 wt% Rh	$\bar{d}$ (nm)		
	$\Delta t = 0^a$	$\Delta t = 10$ min	$\Delta t = 2$ h
Al_2O_3	1.1	2.7	4.5
YSZ	2.5	2.7	2.8
TiO_2	1.5	1.8	2.9
MgO	2.2	2.3	2.5

[a] Values correspond to fresh catalyst samples before their exposure to the reaction mixture at 650°C.

reaction conditions accounts, at least partially, for the reduction of methane conversion with time on stream.

In addition to carbon deposition and metal sintering, participation of the catalyst carrier via solid phase reactions with metallic sites to form less active centers, or migration of species from the carrier onto the metallic surface, blocking, therefore, active sites may also contribute to catalyst deactivation. Concerning these aspects, the Rh/TiO_2 catalyst was of special concern since this catalyst is capable of exhibiting the SMSI phenomenon (22). The H_2 TPD technique, as described in a previous paragraph, was applied to estimate the variation of exposed Rh surface area of Rh/TiO_2 catalyst with time on stream. However, unlike the methodology described above (Table 3), the step of O_2 treatment at 650°C was not applied since this step destroys the SMSI state and recovers the H_2 chemisorption capacity (23). Thus, the catalyst after reaction at 650°C for 2 h was purged with He at 650°C for 3 min and was then quickly cooled to room temperature for direct H_2 chemisorption. Figure 7 compares the two H_2 TPD spectra with and without the step of O_2 treatment at 650°C. It is shown that the capacity for H_2 chemisorption of the catalyst not treated with O_2 at 650°C after reaction (curve (b)) is much lower than that obtained after O_2 treatment at 650°C, following reaction (curve (a)). A decrease of H_2 chemisorption by approximately 40% is noted. Since carbon deposition on the Rh/TiO_2 catalyst under the same reaction conditions is very small ($\theta_C = 0.007$), this cannot account for the differences in H_2 uptake shown in Fig. 7. Thus, the reduction of H_2 uptake of the working catalyst surface, which has not been exposed to O_2, can be attributed to induction of the SMSI state under reaction conditions. After destruction of the SMSI state by oxygen treatment, followed by a low-temperature H_2 reduction (at 300°C), it was found that the capacity of the supported Rh crystallites for H_2 chemisorption was essentially recovered. These results seem reasonable considering that the reaction temperature is high (650°C) and the products of the reaction (H_2/CO) are reducing gases. Thus, it can be stated that participation of the catalyst carrier (TiO_2) via the SMSI phenomenon also contributes to catalyst deactivation. A reduction of activity in the CO_2/H_2 reaction under the SMSI state has also been observed over the present Rh/TiO_2 catalyst (24).

The Rh/MgO is one of the catalysts which exhibit high deactivation rates (Table 2). However, neither carbon deposition nor sintering of the metal crystallites can account entirely for the deactivation of this catalyst, as was demonstrated above. Thus, the possibility of participation of the carrier in the process of deactivation was explored. Unlike the case of reducible oxide carriers, such as TiO_2, for which deactivation can be partially attributed to the SMSI phenomenon, other surface processes involving participation of the carrier should be sought in the case of the Rh/MgO catalyst. Figure 8 shows H_2 TPD spectra over the Rh/MgO catalyst following H_2 chemisorption after different gas pretreatments. In Fig. 8a, two main H_2 peaks are registered following H_2 chemisorption at 300°C for 0.5 h, cooling in H_2 flow to 30°C, and maintaining for 0.5 h, over a fresh sample. A major peak is recorded at 210°C, and a smaller one at 80°C. A very different spectrum (Fig. 8b), however, was obtained on the sample which had been reduced in H_2 flow at 500°C for 1 h followed by the same H_2 adsorption procedure as for Fig. 8a. While no H_2 peak is observed in the temperature range 30–390°C, a small H_2 peak evolves at higher temperatures ($T_M = 510$°C). The large decrease in H_2 chemisorption, upon high temperature reduction, appears to be due to poisoning of Rh surface by species which originate from the MgO carrier. Note that the Rh particle size of Rh/MgO did not significantly alter after high temperature treatment, as shown in Table 3. When

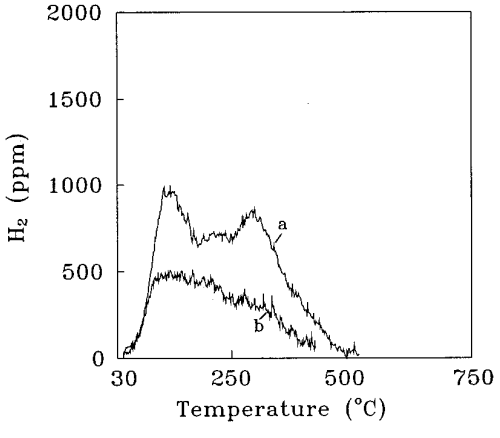

FIG. 7. Temperature-programmed desorption (TPD) of H_2 from the 0.5 wt% Rh/TiO_2 catalyst following reaction with CH_4/CO_2 at 650°C for 2 h. (a) after reaction → O_2/He (650°C, 20 min) → H_2 (300°C, 1 h) → cooling in H_2 at 30°C and a stay for 30 min → He (30°C, 5 min) → TPD; (b) after reaction → He (650°C, 5 min) → H_2 (300°C, 1 h) → cooling in H_2 at 30°C and a stay for 30 min → He (30°C, 5 min) → TPD.

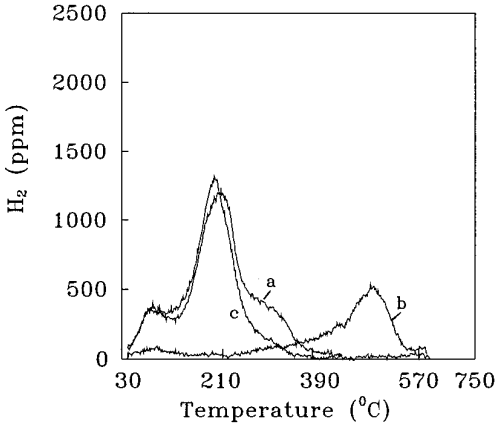

FIG. 8. Temperature-programmed desorption (TPD) of H_2 from the 0.5 wt% Rh/MgO catalyst. Gas delivery sequence: (a) fresh sample → 30 min H_2 at 300°C → 30 min H_2 at 30°C → 5 min He at 30°C → TPD; (b) 1 h H_2 at 500°C → 30 min H_2 at 300°C → 30 min H_2 at 30°C → 5 min He at 30°C → TPD; (c) 1 h H_2 at 500°C → 30 min O_2 at 450°C → 1 h H_2 at 300°C → 30 min H_2 at 30°C → 5 min He at 30°C → TPD.

the Rh/MgO surface was treated in O_2 flow at 450°C for 30 min, after the H_2 TPD of Fig. 8a, followed by reduction in H_2 flow at 300°C, a complete recovery of the capacity for H_2 chemisorption was observed as indicated in Fig. 8c. This spectrum is similar to that obtained over the fresh sample (compare Figs. 8a and 8c). H_2 chemisorption on Rh/MgO catalyst has been investigated in previous studies (25, 26). It was found that a large decrease in H_2 chemisorption occurred on Rh/MgO after various temperature treatments in H_2, and the initial capacity could be recovered by oxidation at 400°C followed by H_2 reduction at low temperature (25). The decrease of H_2 chemisorption was attributed to blockage of Rh surface sites by sulfate, originating from the MgO support which contained sulfur impurities. This attribution was supported by the fact that suppression of H_2 chemisorption and recovery by O_2 treatment did not exist when ultrapure MgO support was employed (25). According to these results, it appears that the reduction in H_2 chemisorption over the present sample, reduced at 500°C, is related to migration of sulfur species from the MgO carrier. Since the reaction temperature applied is high (650°C) and the working catalyst is exposed to a rather reducing atmosphere (H_2, CO, and CH_4), it is likely that sulfur species gradually migrate from the MgO support onto the Rh surface under reaction conditions leading to catalyst deactivation by blockage of surface Rh sites.

(*b*) *Integral Reactor Performance*

The catalytic performance of Rh dispersed on SiO_2, γ-Al_2O_3, and TiO_2 carriers was investigated under integral reactor conditions within the temperature range 600 to 750°C. Conversions and selectivities close to those expected at thermodynamic equilibrium were achieved in all cases. It is of interest to note that the conversion of CO_2 was always higher than the conversion of CH_4, although a feed ratio of unity was used. The difference was more pronounced at low temperatures. Significant quantities of water were observed when the reaction was carried out at low temperatures, while only trace amounts were detected at high reaction temperatures. Furthermore, the selectivity towards CO formation was always higher than the selectivity towards H_2. These observations imply that in addition to the main CO_2 reforming reaction, the reverse water–gas shift reaction is also taking place.

It was shown in a previous section that some of the present supported Rh catalysts deactivate substantially at 650°C (Table 2). However, other studies in our laboratory have indicated that the degree of deactivation is reduced when the reaction takes place at higher temperatures. Therefore, attention was focused to investigate the long-term stability of various supported rhodium catalysts at temperatures higher than 650°C.

The long-term stability performance of 0.5 wt% Rh/SiO_2, γ-Al_2O_3, TiO_2 and YSZ catalysts was examined at 750°C. Figure 9 shows results of CH_4 conversion as a function of time on stream over three of the catalysts at 750°C with a feed containing 20% CH_4, 20% CO_2, and 60% He. It is apparent that the long-term stability of the Rh/SiO_2 and Rh/YSZ catalysts are the best among the three catalysts and exhibit essentially no deactivation under the conditions employed in this test. For the Rh/TiO_2 catalyst the deactivation rate is initially high but becomes less significant after about 10 h of reaction. The difference between the conversion over the fresh catalyst (after 10 min of reaction) and that obtained after 50 h on stream is as high as 30 percentage units for the Rh/TiO_2, while in the case of Rh/γ-Al_2O_3 (not shown in Fig. 9) only several percentage units. The deactivation rates of these four catalysts show the following order: Rh/TiO_2 $\gg$ Rh/Al_2O_3 $>$ Rh/SiO_2 $\cong$ Rh/YSZ.

The good stability of the Rh/SiO_2 catalyst appears to be related to the inertness of the SiO_2 support, which is capable of exhibiting only a weak or no metal–support interaction. The poor stability of the Rh/TiO_2 catalyst is probably due to the reducibility of the TiO_2 carrier which is capable of exhibiting a strong metal–support interaction. The latter has been demonstrated in a previous section (see Fig. 7). A correlation between the extent of metal-support interaction and deactivation rate seems to exist.

DISCUSSION

(*a*) *Support and Dispersion Effects on Reforming Activity*

The present work reveals that the catalytic performance of supported Rh catalysts for the reforming reaction of

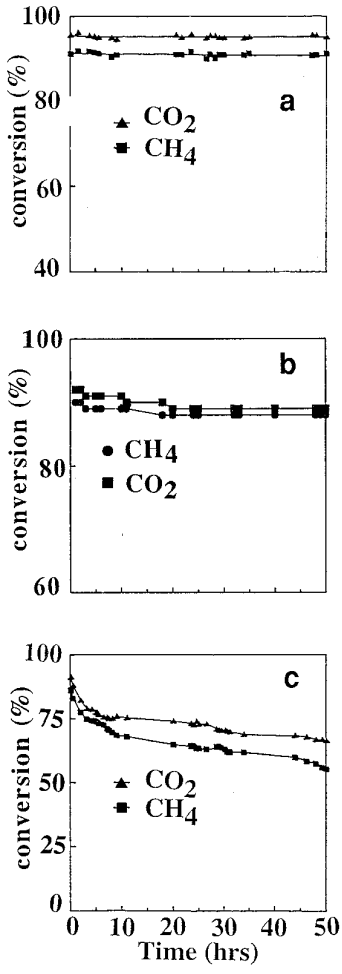

FIG. 9. Variation of methane and CO_2 conversion with time on stream over (a) 0.5 wt% Rh/SiO_2, (b) 0.5 wt% Rh/YSZ, and (c) 0.5 wt% Rh/TiO_2 catalysts. $T = 750°C$; $m_{cat} = 200$ mg; $F_{tot} = 100$ ml/min; $CH_4/CO_2/He = 20/20/60$ mol%.

methane with CO_2, in terms of initial specific activity and CH_4 conversion, is strongly influenced by the support employed to disperse the active metal component. The TOF results shown in Table 1 reveal that the methane reforming activity of Rh decreases in the following order: YSZ > $Al_2O_3 \geq TiO_2 > SiO_2 > La_2O_3 > MgO$. It is also shown that the highest rate, obtained over the Rh/YSZ, is approximately 80 times larger than the rate obtained over the Rh/MgO. It must be emphasized that the results reported in Table 1 represent initial ($t = 0$) activities, free of any deactivation processes. The present results are in agreement with those of Nakamura *et al.* (17), who observed an activity order of $Rh/Al_2O_3 > Rh/TiO_2 > Rh/SiO_2$. However, an earlier study by Erdöhelyi *et al.* (15) failed to observe any significant carrier effect on the activity of supported Rh for CH_4 reforming with CO_2 at 500°C.

A comparison of the initial activity (TOF) and of the acidity of the carriers reveals that a correlation between TOF and surface acidity seems to exist; i.e., the higher the acidity the higher the initial reaction rate. Recent studies in this laboratory have shown that a similar correlation also exists for supported Ru catalysts for the same reaction. Although the intrinsic reason for such a correlation is presently unclear, it appears that the acidic nature of the carrier may promote methane dissociation, probably via $CH_4 \rightarrow CH_3^+ + H^-$, on the sites at the periphery of the metal crystallites (metal-support interface), as suggested by Huder (27). It is known that methane activation favorably occurs on sites with strong acidity via CH_3^+ intermediate species (28, 29).

In the cases of Rh/TiO_2 and Rh/Al_2O_3 catalysts, the reaction appears to be structure sensitive, i.e., the specific activity is affected by the average Rh particle size (Fig. 1). The extent of structure sensitivity is also found to depend on the nature of the support. However, the reforming reaction over the Rh/SiO_2 catalyst appears to be facile, i.e. the specific activity is not significantly affected by the average Rh particle size (Fig. 1). These results tend to suggest that indeed the reforming reaction over Rh crystallites must be treated as a facile reaction, while the dependence of TOF on Rh particle size, when Rh is supported on TiO_2 or Al_2O_3, is due to some direct or indirect interaction of the support with the Rh crystallites. This view is supported by the results shown in Fig. 1 which show that large alterations of TOF occur in the particle size range 1–2.5 nm, while for 5.0 nm Rh particle size the TOF value is more or less the same, independent of the support. In other words, the higher the dispersion, the higher the metal–support interfacial area, which results in metal-support interactions of higher intensity. In addition, in the case of the Rh/TiO_2 system, the higher the Rh dispersion the larger the extent of the SMSI phenomenon is expected. It should be noted that the SMSI state could be induced prior to initiation of the reaction, during H_2 treatment or heating-up of the catalyst.

In spite of the fact that a significant amount of carbon is formed during reaction over the Rh/Al_2O_3 catalyst (Fig. 3, Table 2), this catalyst exhibits high TOF values as compared to the other supported Rh catalysts (Table 1). This result could be related to the amount of active carbon species which participate in the sequence of steps to form CO. In Part 2 of this work (18), it is illustrated, through steady-state tracing experiments, that the amount of active carbon over the Rh/Al_2O_3 system corresponds to a surface coverage value of 0.2, while over the Rh/TiO_2, Rh/YSZ, and Rh/MgO catalysts it is partically immeasurable ($\theta_C < 0.01$). The higher TOF value obtained over the Rh/YSZ catalyst as compared to that of Rh/TiO_2 (Table 1), for both of which catalysts the amount of active carbon was immeasurable (18), may be due to the larger rate constant k of the rate-limiting step of CO formation (i.e., CH_x +

$O \xrightarrow{k} CO + xH$). This rate constant is associated with the reactivity of both CH_x and O adsorbed species. Steady-state tracing experiments reported in Part 2 of this work (18) over the Rh/YSZ catalyst suggested that lattice oxygen species of the YSZ support participate in the formation of CO during reforming reaction. It is likely, then, that the highest TOF value observed over Rh/YSZ as compared to the other catalysts (Table 1) is partly due to the presence of very active oxygen species derived from the support.

In comparing the large differences in TOF among Rh/YSZ and Rh/MgO, it could be stated that sulfur poisoning might be partly responsible for the very low TOF value of the Rh/MgO catalyst. If sulfur is indeed migrating onto the metallic sites, as the H_2 chemisorption results of Fig. 8 suggest, this could be taking place during reduction of the catalyst and during heating, prior to initiation of the reaction. This result is strongly against the alternative explanation that H_2S of less than 1 ppm (not presently detected) in the feed stream could strongly affect the reaction rate by blockage of Rh surface area within the first few minutes of the reaction. The phenomenon of sulphur poisoning could also explain the difference in reactivity order with respect to the carrier between the present study and the work of Erdöhelyi *et al.* (15). The latter authors observed that the Rh/MgO catalyst exhibited the highest TOF value among other supports investigated.

The effect of alkali surface promotion on catalytic rates is a well-known phenomenon. Small amounts of such promoters on the metallic surface can cause large changes in the intrinsic catalytic activity. In the present work alkali impurities (i.e., K^+ and Na^+) could originate from the various supports used, which were all commercial ones. This work did not go into a detailed surface analysis of the fresh and spent catalysts in order to examine the possibility of having promotional effects from alkali impurities of the supports used. Therefore, the conclusions reached concerning relative specific activities of the series of supported Rh catalysts investigated do not address the issue of any surface promotional effects due to alkali impurities, if any, in the support used.

(*b*) *Support Effects on Catalyst Deactivation*

The rates of deactivation observed over Rh crystallites supported on various carriers are found to be largely different (Fig. 2, Table 2). For the case of γ-Al_2O_3, SiO_2, and TiO_2 there also exists a particle size effect on the rate of deactivation, which is larger in the case of Rh/TiO_2 catalyst. As has been demonstrated in the Results section, the causes of deactivation of Rh supported on TiO_2, Al_2O_3, YSZ, and MgO are different. Three types of deactivation processes have been probed, namely, (a) carbon deposition, (b) metal sintering, and (c) poisoning of Rh active sites by species originating from the support via spillover. The importance of each process is found to depend on the nature of the support and the size of the Rh particles.

In the Rh/Al_2O_3 catalyst, after 2 h of exposure of the fresh sample to the CH_4/CO_2/He stream at 650°C, the particle size of Rh is found to be about 4.5 nm, as compared to 1.1 nm for the fresh sample (Table 3), while in the cases of Rh/TiO_2, Rh/YSZ, and Rh/MgO the Rh particle size after 2 h of reaction at 650°C is approximately the same ($\bar{d} \cong 2.8$ nm, Table 3) for all three catalysts. Note also that over these three catalysts the amount of carbon formed during the reforming reaction is negligibly small (Table 2). These results may suggest that the accumulation of carbon in larger quantities over the Rh/Al_2O_3 is likely to be the result of some interaction of Rh crystallites with the alumina surface which influences carbon formation and removal reaction steps.

Transient isotopic experiments to be presented in Part 2 of this work (18) indicate that the accumulated carbon during the reforming reaction over the Rh/Al_2O_3 catalyst is mainly derived from the CO_2 molecule. An accepted mechanism for carbon deposition based on the CO_2 molecule is via the following dissociation steps:

$$CO_2 + 2s \rightarrow CO - s + O - s \quad [1]$$

$$CO - s + s \leftrightarrows C - s + O - s. \quad [2]$$

Here (s) is a site on the Rh surface or along the metal–support interface. According to these reaction steps and what was mentioned in the previous paragraph, the dependence of both CO_2 and CO dissociation steps on the nature of the site (s), i.e., a site on the Rh surface versus a site along the metal–support interface, could explain the differences in carbon deposition among the present supported Rh catalysts (see Table 2). On the other hand, other reaction steps of carbon removal may also be considered as sensitive to the nature of the site(s), such as

$$H_2O + 2s \rightarrow OH - s + H - s \quad [3]$$

$$C - s + OH - s \rightarrow CO - s + H - s. \quad [4]$$

Che and Bennett (30) in their review paper report that the rate of carbon deposition from the disproportionation step of CO decreases with increasing metal particle size over Ni/mica, Pd/mica, Pd/SiO_2, and Fe/C catalysts. No information is provided for supported Rh catalysts. On the other hand, Efstathiou *et al.* (31) have found that over the Rh/Al_2O_3 catalyst the amount of carbonaceous species C_xH_y formed on the Rh surface during the CO/H_2 reaction increases with increasing Rh particle size ($\bar{d}$ = 1.5 vs 9.0 nm); it should be noted that the CO dissociation step (2) is responsible for the formation of these C_xH_y species. It is speculated whether the latter results may support the present results of enhanced carbon deposition over the

larger Rh particles ($\bar{d}$ = 4.5 nm) supported on Al_2O_3 as compared to reduced carbon deposition on smaller Rh particles supported on MgO, TiO_2, and YSZ ($\bar{d}$ = 2.8 nm). It is also speculative whether the CO_2 dissociation step [1] might be considered as structure sensitive, where an enhanced dissociation rate is found with increasing Rh particle size.

It is found in the present work that neither significant carbon deposition nor substantial metal sintering occurs over the Rh/YSZ and Rh/MgO catalysts. The deactivation observed over these two catalysts should, therefore, be mainly attributed to other surface processes which may involve participation of the carrier. Evidence has been presented that catalyst deactivation over the Rh/TiO_2 and Rh/MgO is caused by species originating from the carrier. In the former case, surface Rh sites are partially blocked by TiO_x species which migrate from the TiO_2 carrier onto the surface, due to the occurrence of the SMSI phenomenon. *In situ* FTIR experiments performed over the present Rh/TiO_2 catalyst showed an infrared band at 2052 cm^{-1}, attributed to linearly adsorbed CO, which first decreased and then disappeared with time on stream. This result may suggest that the surface Rh sites are gradually covered by TiO_x species originating from the support in agreement with the H_2 TPD results of Fig. 7. In the case of Rh/MgO, surface Rh sites may be blocked by sulfur species originating from the MgO carrier, as has already been mentioned in the Results Section.

It should be pointed out that, in addition to the three major factors described above which cause catalyst deactivation, there is another important factor which could be considered as leading to catalyst deactivation. This is the accumulation of inactive (strongly bound) adsorbed oxygen species originating either from the support or from the dissociation of CO_2 and CO on the metallic surface. However, unlike nonnoble metals (e.g., Co, Fe, Ni) the stability of oxygen adatoms on a noble metal, particularly Rh, is rather poor at high temperatures (32, 33). The coverage of oxygen adatoms on supported Rh catalysts is expected to be small under reaction conditions (high temperatures and reducing atmosphere), unless there is a different oxygen source such as the carrier (the case of the Rh/YSZ catalyst) in which strongly bound oxygen could be formed at the periphery of the Rh surface and the YSZ support. These views are supported by transient isotopic results which are presented in Part 2 of this work (18).

(*c*) *Chemical Nature of Carbonaceous Species Measured by TPO and TPH Experiments*

Temperature-programmed oxidation (TPO) and hydrogenation (TPH) experiments allowed the measurement of carbonaceous species formed after reforming reaction at 650°C and their characterization towards oxidation to CO_2 and hydrogenation to methane and ethane (Figs. 3, and 4, 5, respectively). On the other hand, these experiments are not appropriate to characterize the chemical nature of these carbonaceous species. In Part 2 of this work (18), *in situ* FTIR experiments and others based on mass spectrometry, which were designed to study the chemical composition of intermediate surface adsorbed species formed during reaction, will be presented. It was found that at 650°C only adsorbed CO on the Rh surface and formate species on the alumina support, in the case of Rh/Al_2O_3 catalyst, are accumulated under reforming conditions. No infrared bands corresponding to $-CH_x$ adsorbed species nor to carbonate/bicarbonate species are formed. In addition, it was found that after an Ar purge at 650°C for 10 min, following reforming reaction, all the adsorbed CO and formate species desorb and decompose, respectively, from the catalyst surface. According to these FTIR results obtained over the Rh/Al_2O_3 catalyst, it becomes clear that the TPO and TPH responses presented in Figs. 3 and 4, respectively, do not correspond to oxidation or hydrogenation of surface CO and formate species, but exclusively to carbon species, the latter not detected by FTIR (i.e., C_xH_y with $y \cong 0$). This assignment is also in harmony with the fact that during the TPO experiment presented in Fig. 3 only very small amounts of water are formed in the temperature range 100–500°C.

The active carbon species hydrogenated to CH_4 at 100°C (Fig. 4), which is also oxidized to CO_2 at the same temperature (Fig. 3), might be of carbidic form, while the other two carbon species identified in the TPH spectrum might be of some kind of carbon chains and graphitic form. Erdöhelyi *et al.* (15) have studied the formation of carbonaceous species during the reforming reaction at 500°C where a C/Rh_s ratio of 0.06 was reported after 1 h of reaction over 1 wt% Rh/Al_2O_3 catalyst. On the other hand, a lower surface carbon coverage was found over Rh supported on TiO_2, MgO, and SiO_2. These results are consistent to the present ones as far as the effect of support on carbon accumulation is concerned. The higher value of C/Rh_s found in the present Rh/Al_2O_3 catalyst as compared to that reported by Erdöhelyi *et al.* (15) is most probably due to the higher reaction temperature used in the present study (T = 650–750°C). A carbon species CH_x ($x \approx 0$) similar in hydrogenation activity formed over the Rh/Al_2O_3 catalyst has been reported by Efstathiou *et al.* (31) for the CO/H_2 reaction. Given the fact that the carbon species formed over this catalyst under CH_4 reforming conditions is derived by the dissociation of CO (see Part 2, Ref. (18)), the sharp peak of CH_4 shown in Fig. 7 is, therefore, not of surprise. Different forms of carbon species derived by the dissociation of CO over the Rh/Al_2O_3 catalyst have also been reported in the past (31, 36).

The CO_2 response obtained during the TPO experiment shown in Fig. 3 reveals four distinct peaks. These peaks

are assigned to different kinds of carbon, in terms of their activity to oxidation. Considering the fact that part of the CO_2 which is initially produced at 100°C could adsorb on the alumina support and then desorb at higher temperatures, the abovementioned assignment of different kinds of carbon species would then be questionable. However, the TPH experiments shown in Fig. 4 reveal three well resolved CH_4 peaks and a shoulder to the left of the second peak (Fig. 4a). Thus, there is a very good agreement between the TPH and TPO experiments concerning the number of carbon species identified based on their reactivities towards hydrogenation and oxidation. Adsorption of CO_2 on the Al_2O_3 support could only alter the relative amounts of the four CO_2 peaks calculated based on the observed response in Fig. 3 but not the total quantity of CO_2 produced from the combustion reaction of carbon species formed under reaction conditions. The amount of carbon species calculated based on the TPH experiments was usually smaller than the amount calculated based on the TPO experiments. These results suggest that part of the carbonaceous species formed at 650°C become inactive towards hydrogenation up to 500°C but active towards oxidation.

The TPH experiment of carbonaceous species formed during the reforming reaction over the Rh/YSZ catalyst (Fig. 5) indicates that significant amounts of ethane, as compared to methane, are formed, a result which is completely different from that obtained over the Rh/Al_2O_3 catalyst (only CH_4 is observed in Fig. 4). These results may suggest that the chemical composition of carbonaceous species formed over the Rh/YSZ catalyst could be of some hydrogenated form of carbon, i.e., $-CH_2$, $-CH_3$, or $-CH_xCH_y$, whose hydrogenation to ethane, in addition to methane, could also be favored. The very small amount of such carbonaceous species did not allow either the FTIR technique nor the TPO technique (via the measurement of H_2O) to investigate the true chemical nature of these species. On the other hand, one cannot exclude the possibility that hydrogenation of atomic carbon to $-CH_x$ species, followed by coupling reaction of $-CH_x$ species and further hydrogenation steps, could also be favored over the Rh/YSZ than over the Rh/Al_2O_3 catalyst. It should be noted that YSZ is a fairly active methane oxidative coupling catalyst (35). The formation of C_2H_6 during hydrogenation of carbon species deposited by CH_4 decomposition over supported Rh catalysts has recently been reported by Erdöhelyi *et al.* (15).

(*d*) *Catalytic Performance of Supported Rh Catalysts*

The most pronounced advantages of catalysts based on noble metals for the reforming reaction of methane with CO_2 are their high activity and good long-term stability, as compared to nickel-based catalysts (9, 11, 12, 34). As has been demonstrated in the present study, the activity and stability of catalysts based on rhodium are still affected, to a large extent, by the nature of the carrier and the metal particle size. These results clearly suggest that an improvement of the catalytic performance of supported Rh catalysts, which are considered to possess relatively high activity and good stability, is still possible.

The reforming reaction in the temperature range 600–750°C, $P_{CH_4} = 0.2$ bar, $CH_4/CO_2 = 1$, and 1 atm total pressure over Rh supported on SiO_2, γ-Al_2O_3, and TiO_2 resulted in CO_2 conversions higher than CH_4 conversions. In addition, the difference in CH_4 and CO_2 conversions was found to decrease with increasing reaction temperature. These results are likely to be due to the reverse water–gas shift reaction:

$$CO_2 + H_2 \leftrightharpoons CO + H_2O. \qquad [5]$$

As reaction temperature increases, CO_2 conversion due to reforming increases, thereby shifting the equilibrium of reaction [5] towards the left. This results in a smaller difference between the CH_4 and CO_2 conversions obtained with increasing reaction temperature. The same arguments apply for the difference in selectivities of the reforming reaction to CO and H_2 which were described in the Results section.

The catalytic results of CH_4 conversion vs. reaction time shown in Fig. 9b obtained over the Rh/Al_2O_3 indicate that over a period of 2 h of reaction the CH_4 conversion does not drop by more than few percentage units. A similar result was obtained under different conditions (21). However, Table 3 indicates that the Rh surface area of the fresh sample (not exposed to the reaction mixture) as compared to that after 2 h of reaction decreases by a factor of 4. One then would expect a similar drop in the activity of the catalyst, which was not observed. This discrepancy is due to the fact that when the catalyst is brought to the reaction temperature of 650°C (following H_2 reduction at 400°C) under He flow, the Rh surface area is already sintered (as found by H_2 TPD and activity measurements). The mean Rh crystallite size reported in Table 3 after 10 min of reaction is indeed similar to that at the start of the reaction at 650°C. In other words, the Rh crystallite size of the fresh sample is not the same as that corresponding to the start of the reaction ($t = 0$).

CONCLUSIONS

The following conclusions can be drawn from the results of the present investigation:

1. The performance of supported Rh catalysts under conditions of methane reforming with CO_2, in terms of initial specific activity, is a strong function of the carrier employed to disperse the metal. The activity decreases in the order $YSZ > Al_2O_3 \geq TiO_2 > SiO_2 > La_2O_3 > MgO$.

2. The initial intrinsic activity of Rh exhibits a dependence on particle size, decreasing with increasing average crystallite size. However, the degree of this dependence is largely affected by the nature of the carrier, suggesting that the dependence of activity on metal particle size might be related to metal–support interactions. No structure sensitivity is observed over the Rh/SiO_2 catalyst.

3. The rate of deactivation over supported Rh catalysts is influenced by the metal particle size. Higher deactivation rates are obtained over smaller Rh particles.

4. The carrier plays an important role on the rate of deactivation. While high deactivation rates are observed over the Rh/TiO_2 and Rh/MgO catalysts, low deactivation rates are observed over the Rh/YSZ, γ-Al_2O_3, La_2O_3, and SiO_2 catalysts. At least three factors contribute to catalyst deactivation, namely, carbon deposition, sintering of metal crystallites, and blocking of the Rh surface sites by species originating from the carrier. The importance of each factor is largely determined by the nature of the carrier.

5. In terms of intrinsic activity and catalyst stability, Rh/YSZ, Rh/SiO_2, and Rh/γ-Al_2O_3 exhibit the best catalytic performance among the other catalysts studied. In the case of Rh/YSZ and Rh/SiO_2, no catalyst deactivation was observed during 50 h of reaction under integral conditions.

ACKNOWLEDGMENT

Financial support by the Commission of the European Community (Contract JOU2-CT92-0073) is gratefully acknowledged.

REFERENCES

1. Gadalla, A. M., and Bower, B., *Chem. Eng. Sci.* **43,** 3049 (1988).
2. Rostrup-Nielsen, J. R., *Stud. Surf. Sci. Catal.* **36,** 73 (1988).
3. Trimm, D. L., *Catal. Rev.—Sci. Eng.* **16,** 155 (1977).
4. Chubb, T. A., *Sol. Energy* **24,** 341 (1980).
5. Dish, J. D., and Hawn, B., *J. Sol. Energy Eng.* **109,** 215 (1987).
6. Fischer, F., and Tropsch, H., *Brennst. Chem.* **3,** 39 (1928).
7. Sodesawa, T., Dobashi, A., and Nozaki, F., *React. Kinet. Catal. Lett.* **12,** 107 (1979).
8. Rudnitskii, L. A., Solboleva, T. N., and Alekseev, A. M., *React. Kinet. Catal. Lett.* **26,** 149 (1984).
9. Gadalla, A. M., and Sommer, M. E., *Chem. Eng. Sci.* **44,** 2825 (1989).
10. Tenner, S., *Hydrocarbon Process* **64,** 106 (1985).
11. Richardson, J. T., and Paripatyadar, S. A., *Appl. Catal.* **61,** 293 (1990).
12. Ashcroft, A. T., Cheetham, A. K., Green, M. L. H., and Vernon, P. D. F., *Nature* **352,** 225 (1991).
13. Solymosi, F., Kutsan, G., and Erdöhelyi, A., *Catal. Lett.* **11,** 149 (1991).
14. Rostrup-Nielsen, J. R., and Bak Hansen, J.-H., *J. Catal.* **144,** 38 (1993).
15. Erdöhelyi, A., Cresényi, J., and Solymosi, F., *J. Catal.* **141,** 287 (1993).
16. Erdöhelyi, A., Cresényi, J., Papp, E., and Solymosi, F., *Appl. Catal. A.* **108,** 205 (1994).
17. Nakamura, J., Aikawa, K., Sato, K. and Uchijima, T., *Catal. Lett.* **25,** 265 (1994).
18. Efstathiou, A. M., Kladi, A., Tsipouriari, V., and Verykios, X. E., *J. Catal.* **158,** 64 (1996).
19. Efstathiou, A. M., Papageorgiou, D., and Verykios, X. E., *J. Catal.* **141,** 612 (1993).
20. Schouten, F. C., Kaleveld, E. W., and Bootsma, G. A., *Surf. Sci.* **63,** 460 (1977); **87,** 1 (1979).
21. Tsipouriari, V., Efstathiou, A. M., Zhang, Z. L., and Verykios, X. E., *Catal. Today* **21,** 579 (1994).
22. Tauster, S. J., and Fung, S. C., *J. Catal.* **55,** 29 (1978).
23. Bonneviot, L., and Haller, G. L., *J. Catal.* **130,** 359 (1991).
24. Zhang, Z. L., Kladi, A., and Verykios, X. E., *J. Catal.* **148,** 737 (1994).
25. Wang, J., Lercher, J. A., and Haller, G. L., *J. Catal.* **88,** 18 (1984).
26. Efstathiou, A. M., *J. Mol. Catal.* **69,** 41 (1991).
27. Huder, K., *Chem. Ing. Tech.* **63,** 376 (1991).
28. Pitsai, P., and Kleir, K., *Catal. Rev.-Sci. Eng.* **28,** 13 (1986).
29. Zhang, Z. L., Verykios, X. E., and Baerns, M., *Catal. Rev.—Sci. Eng.* **36,** 507 (1994).
30. Che, M., and Bennett, C. O., *in* "Advances in Catalysis," Vol. 36, Academic Press, 1989.
31. (a) Efstathiou, A. M., and Bennett, C. O., *J. Catal.* **120,** 118 (1989); (b) Efstathiou, A. M., and Bennett, C. O., *J. Catal.* **120,** 137 (1989); (c) Efstathiou, A. M., Chafik, T., Bianchi, D., and Bennett, C. O., *J. Catal.* **148,** 224 (1994).
32. Winkler, A., Guo, X., Siddiqui, P. L., Hagans, P. L., and Yates, J. T., Jr., *Surf. Sci.* **201,** 419 (1988).
33. Hickman, D. A., Haupfear, E. A., and Schmidt, L. D., *Catal. Lett.* **17,** 223 (1993).
34. Zhang, Z. L., and Verykios, X. E., *Catal. Today* **21,** 589 (1994).
35. Seimanides, S., Tsiakaras, P., Verykios, X. E., and Vayenas, C. G., *Appl. Catal.* **68,** 40 (1991).
36. Erdöhelyi, A., and Solymosi, F., *J. Catal.* **84,** 446 (1983).